

Spectral Analysis of the Ly α Forest Using Wavelets

A. Meiksin

*Institute for Astronomy, University of Edinburgh,
Blackford Hill, Edinburgh EH9 3HJ, UK*

Accepted 1999 December 17. Received 1999 July 26

ABSTRACT

It is shown how wavelets may be used to analyse the absorption properties of the Ly α forest. The Discrete Wavelet Transform of a QSO spectrum is used to decompose the light fluctuations that comprise the forest into orthogonal wavelets. It is demonstrated that most of the signal is carried by the moderate to lower frequency wavelets in high resolution spectra, and that a statistically acceptable description of even high signal-to-noise spectra is provided by only a fraction (10–30%) of the wavelets. The distributions of the wavelet coefficients provide a statistical basis for discriminating between different models of the Ly α forest. The method is illustrated using the measured spectrum of Q1937–1009. The procedure described is readily automated and may be used to process both measured spectra and the large number of spectra generated by numerical simulations, permitting a fair comparison between the two.

Key words: intergalactic medium – methods:data analysis – quasars:absorption lines

1 INTRODUCTION

Measurements of QSO spectra show that the Intergalactic Medium (IGM) is composed of highly inhomogeneous structures. Ever since their identification by Lynds (1971) and the pioneering survey of Sargent et al. (1980), these inhomogeneities have been described as discrete absorption systems, the Ly α forest. With the view that the systems arise from individual intervening gas clouds, the Ly α forest has been characterized using traditional absorption line statistics, most notably the line equivalent widths and, as the spectra improved in resolution and signal-to-noise ratio, the Doppler widths and H I column densities through Voigt profile line fitting to the features.

In the past few years, numerical simulations have successfully modelled many of the measured properties of the forest, showing that the absorption systems may arise as a consequence of cosmological structure formation (Cen et al. 1994; Zhang, Anninos & Norman 1995; Hernquist et al. 1996; Bond & Wadsley 1997; Zhang et al. 1997; Theuns, Leonard & Efstathiou 1998). The simulations have shown, contrary to the picture in which the systems are isolated intergalactic gas clouds, that most of the systems originate in an interconnected web of sheets and filaments of gas and dark matter (Cen et al. 1994; Bond & Wadsley 1997; Zhang et al. 1998). Alternative statistical methods were subsequently introduced for describing the forest using the more direct measurements of the induced light fluctuations. These include the 1-point distribution of the fluctuations (Miralda-Escudé et al. 1996; Zhang et al. 1997), and a quantity related to the 2-point distribution based on a

weighted difference of the light fluctuations in neighbouring wavelength pixels (Miralda-Escudé et al.). A direct estimate of the 2-point transmission correlation function was made by Zuo & Bond (1994).

While the newer methods for analysing the Ly α forest avoid the identification of absorption lines and the fitting of Voigt profiles, they are not necessarily fundamentally different in their description of the spectra. For instance, Zhang et al. (1998) find that the distribution of optical depth per pixel in their simulation may be recovered by modelling the spectra entirely by discrete absorption lines with Voigt profiles. Rather the more direct methods circumvent a difficulty that has long plagued attempts to characterize the absorbers in terms of Voigt profiles: the sensitivity of the resulting line statistics to noise and to the fitting procedure. Absorption line fitting of necessity requires arbitrary decisions to be made regarding the setting of the continuum level, the deblending of features, and a decision on the acceptability of a fit. Different observational groups report different distributions for the line parameters. Most discrepant has been the inferred distribution of line widths. Even with the highest quality data gathered to date using the Keck HIRES, agreement is still lacking, with Hu et al. (1995) finding a narrower Doppler parameter distribution with a significantly higher mean than found by Kirkman & Tytler (1997). The differences are important, as cosmological simulations predict comparable differences for a range of plausible cosmological models (Machacek et al. 2000; Meiksin et al. 2000).

The purpose in this paper is to develop a method that provides an alternative objective description of the statistics of the Ly α forest. Ultimately the goal is to employ the same

method for analysing both observational data and data derived from numerical simulations in order to compare the two on a fair basis. Because of the large number of synthetic spectra generated from a simulation necessary to provide a correct average description of the forest, two principal requirements of the procedure are that it be fast and easily automated. Although automated or semi-automated Voigt profile fitting procedures exist (AutoVP, Davé et al. 1997; VPFIT, developed by Carswell and collaborators), these procedures still require arbitrary decisions to be made to obtain acceptable fits. The complexity of the codes makes it difficult to assess the statistical significance of differences between the measured distributions of the absorption line parameters and those predicted. The codes also are computationally expensive, making very costly their application to the large number of simulated spectra required to obtain a statistically valid average of the line parameters. For these reasons, a faster less complex method would be desirable. The Voigt profile fitting codes yield important parameters, like the linewidths, which contain physical information (eg, gas temperature and turbulent velocities), that the direct-analysis methods do not. It would thus be desirable for an alternative method to retain some of this information. The method presented here utilizes wavelets to characterize the absorption statistics of the Ly α forest. It is not intended to be a replacement for Voigt profile fitting, but a fast alternative that allows a ready comparison between the predictions of numerical models and measured spectra and a clear statistical analysis of the results.

The outline of the paper is as follows: in §2 it is shown how the statistics of the Ly α forest may be characterized using wavelets. In §3 the method is applied to the measured spectrum of a high redshift QSO. The results are summarized in §4.

2 ANALYSING THE Ly α FOREST WITH WAVELETS

2.1 Terminology

Although wavelets have been used in signal processing, image analysis, and the study of fluid dynamics for a decade, they are only beginning to enter the vernacular of astronomers. Accessible introductions are provided in Press et al. (1992), and in Slezak, Bijaoui & Mars (1990) and Pando & Fang (1996), who apply wavelets to study the clustering of galaxies and Ly α absorbers, respectively. More complete accounts of wavelet methodology are Chui (1992), Daubechies (1992), and Meyer (1993). The description here is confined to those elements necessary to introduce the notation and terminology that will be used below.

Wavelets are defined variously in the literature. The definition of most use here, somewhat restrictive but appropriate to a multiresolution analysis using the Discrete Wavelet Transform (DWT), is (Meyer):

A *wavelet* is a square-integrable function $\psi(x)$ defined in real space such that $\psi_{jk} \equiv 2^{j/2}\psi(2^j x - k)$, where j and k are integers, is an orthonormal basis for the set of square-integrable functions.

The wavelet $\psi(x)$ satisfies $\int_{-\infty}^{\infty} dx \psi(x) = 0$, and is generally chosen to be concentrated near $x = k2^{-j}$. Its defining properties permit it to perform two operations governed by the

values of j and k . Smaller values of j correspond to coarser variations in $f(x)$, while differing values of k correspond to shifting the centre of the transform.

The *wavelet coefficients* of a function $f(x)$ are defined by

$$w_{jk} \equiv \int dx f(x)\psi_{jk}(x). \quad (1)$$

The set of coefficients $\{w_{jk}\}$ comprises the wavelet transform of the function $f(x)$. The function may then be recovered through the inverse transform

$$f(x) = \sum_{j,k} w_{jk}\psi_{jk}(x), \quad (2)$$

since the set of functions ψ_{jk} forms a complete orthonormal basis. The wavelet coefficients at a level j express the changes between the smoothed representations of $f(x)$ at the resolution scales $j + 1$ and j .

Several functions may serve as wavelets. A set that has proven particularly useful was developed by Daubechies (Daubechies 1992). These functions are constructed to have vanishing moments up to some value p , and the functions themselves vanish outside the range $0 < x < 2p + 1$. The wavelet coefficients decrease rapidly with p for smooth functions. Accordingly, the higher order Daubechies wavelets are the most suitable for analyzing smooth data. The DWT is computed using the pyramidal algorithm as implemented in Numerical Recipes (Press et al.). The Daubechies wavelet of order 20 is chosen throughout.

2.2 Monte Carlo simulations

The properties of the wavelet transform of the Ly α forest are examined by performing Monte Carlo realizations of spectra. The spectra are constructed from discrete lines with Voigt profiles using the H I column density and Doppler parameter distributions found by Kirkman & Tytler. Specifically, the H I column densities N_{HI} are drawn from a power law distribution of slope 1.5 between $12.5 < \log_{10} N_{\text{HI}} < 16$ and the Doppler parameters b from a gaussian with mean 23 km s^{-1} and standard deviation 14 km s^{-1} . A cut-off in b is imposed according to $b > 14 + 4(\log_{10} N_{\text{HI}} - 12.5) \text{ km s}^{-1}$. The resulting average Doppler parameter is 31 km s^{-1} . The number density of lines per unit redshift matches that of Kirkman & Tytler at $z = 3$. The resolution is set at $\lambda/d\lambda = 5 \times 10^4$, and gaussian noise is added according to a specified continuum signal-to-noise ratio per pixel. This is the fiducial model used in all the simulations unless stated otherwise. Segments 128 pixels wide were found adequate for extracting the statistical properties of the wavelet coefficients.

A representative spectrum and its discrete wavelet transform are shown in Figure 1. A block at resolution j is $128/2^j$ pixels wide and 2^j pixels long for $j = 1$ to 6. The resolution becomes finer as j increases from 1 to 6 (downwards). The uppermost level ($j = 0$) corresponds to smoothed averages of the spectrum. The wavelet coefficients tend to increase in magnitude with decreasing resolution (decreasing j). The low values indicate that only small changes occur in the spectrum when smoothed at one resolution level to the next higher. The small values are desirable, as they signify

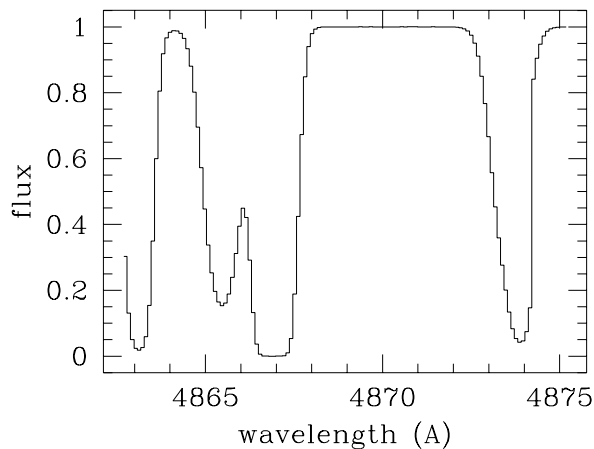


Figure 1. (a) A representative synthetic spectrum showing the Ly α forest at $z = 3.0$ at a resolution of $\lambda/d\lambda = 5 \times 10^4$. (b) The absolute magnitudes of the wavelet coefficients are shown in the grayscale map. The map is linear and ranges between 0 (white) and 0.5 (black).

the dominant absorption features in the spectra are adequately resolved.

Because the wavelet functions form a complete set of basis functions, the full set of wavelet coefficients completely describes the spectrum: the spectrum may be reconstructed identically from the inverse transform. For noisy spectra, however, it will generally be unnecessary to retain the full set of coefficients. Indeed, this is the motivation for multi-resolution data compression. By employing a judicious set of basis functions, a signal may be compressed into only a small fraction of its original size. The method of choosing the optimal basis set such that the compressed signal matches the original as closely as possible in a least squares sense with the least number of retained basis elements is known as Proper Orthogonal Decomposition or the Karhunen–Loève procedure (see Berkooz, Holmes & Lumley 1993 for a review). The basis set, however, will in general differ from signal to signal if its components are highly variable, as in the case of the Ly α forest. Although not optimal in the least squares sense, the wavelet basis nonetheless achieves a large amount of data compression and has the advantage of generality. Next is described how wavelets may be applied to assessing the amount of useful information in a spectrum.

Two measures of the information content of a noisy spectrum are considered, one based on χ^2 and the second on entropy. If $s(x_i)$ is the original spectrum defined at N points x_i (eg, wavelength or velocity), and $s_n(x_i)$ is the spectrum reconstructed from the n largest (in magnitude) wavelet coefficients, then

$$\chi^2 = \sum_{i=1}^N \left[\frac{s(x_i) - s_n(x_i)}{\sigma_i} \right]^2 \quad (3)$$

where σ_i is the measurement error associated with pixel

i. For gaussian distributed measurements, the expectation value of χ^2 is the number of degrees-of-freedom. If n wavelet coefficients are retained, the number of degrees-of-freedom is $N - n$. (Hence, for example, $\chi^2 = 0$ is expected for $n = N$.) The reduced $\chi_{\text{red}}^2 = \chi^2 / (N - n)$ then defines the optimal value of n for truncating the wavelet coefficients.

The information content may also be expressed in terms of the wavelet coefficients directly as an “entropy”^{*}

$$S = - \sum_{jk} \alpha_{jk}^2 \log \alpha_{jk}^2, \quad (4)$$

where the α_{jk} are the normalized coefficients

$$\alpha_{jk} = \frac{w_{jk}}{\left(\sum_{jk} w_{jk}^2 \right)^{1/2}}. \quad (5)$$

This quantity behaves like a physical entropy in the sense that it is maximum when the signal is completely random so that the full set of coefficients $\{w_{jk}\}$ is required to describe it, while it vanishes when the signal may be entirely described by a single coefficient.

The reduced χ^2 for an ensemble of Monte Carlo realizations is shown in Fig. 2 as a function of the fraction $(N - n)/N$ of the wavelet coefficients discarded. As the signal-to-noise ratio per pixel increases, the value of χ_{red}^2 for a given n increases. In all cases, however, there is some $n < N$ for which $\chi_{\text{red}}^2 = 1$. This suggests that an acceptable fit to a noisy spectrum may be provided by only a fraction n/N of the full set of coefficients, with the fraction required increasing as the noise level decreases.

The entropy S is shown in Figure 3. The entropy stays nearly constant out to $\chi_{\text{red}}^2 = 1$, indicating that little information has been lost by discarding the small coefficients. As χ_{red}^2 increases, eventually the entropy decreases as information is lost. Due to the greater information content of the less noisy spectra, as the noise level is decreased, the entropy remains constant to increasingly higher values of χ_{red}^2 before declining.

2.3 Statistics of the wavelet coefficients

It was shown above how wavelets may be used to characterize the noise properties of a spectrum. The wavelet coefficients, however, may also be used to characterize the statistics of the Ly α forest itself.

The distributions of the coefficients (in absolute value) for the several resolution levels are shown in Fig. 4 for a set of simulated spectra with $S/N = 50$, typical of the Keck HIRES spectra. The number of coefficients at a level j is 2^j , with $j = 1$ corresponding to the coarsest resolution, and $j = 6$ to the finest for the $2^7 = 128$ pixels used in a spectrum. The finest resolution ($j = 6$) curve is the steepest. As the resolution becomes increasingly coarse, the amplitude of the coefficients increases, as was found in Fig. 1. This indicates that most of the information in the spectrum is carried by the coarser levels (as well as by the two coarse scale averages, not shown). The finest level has resolved the spectral structures, with little difference between the smoothed representations of the spectrum at resolution levels $j = 5$ and

^{*} Meyer (1993) defines the entropy to be the exponential of S .

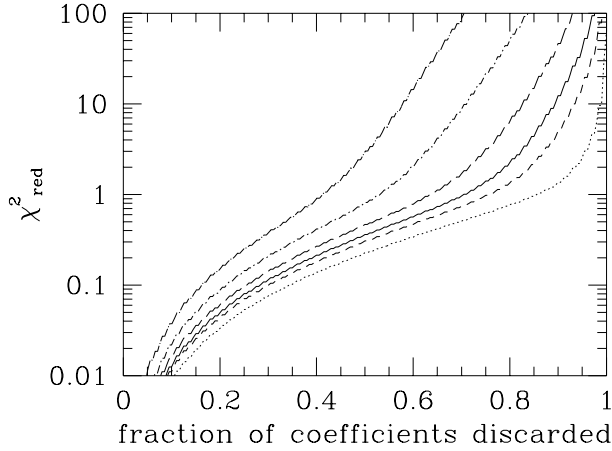


Figure 2. The dependence of the reduced χ_{red}^2 on the fraction of discarded wavelet coefficients. The curves increasing from the bottom are for signal-to-noise ratios of 10, 30, 50, 100, 300, and 1000. As the noise level increases, an increasing fraction of the coefficients may be discarded with the remainder still providing a statistically acceptable fit to the spectra.

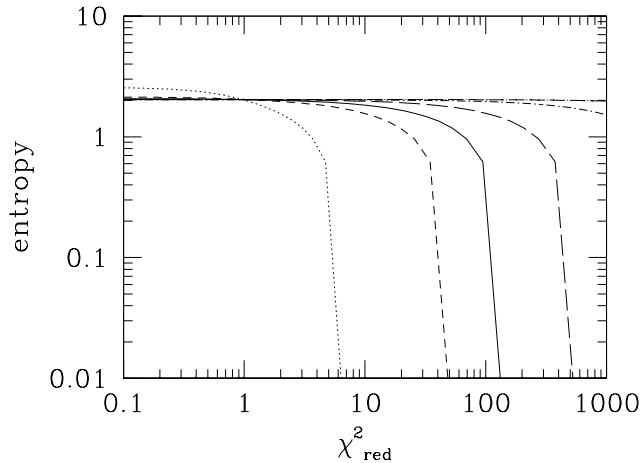


Figure 3. The entropy of the spectra defined in terms of the wavelet coefficients. Little information is lost from the spectra for $\chi_{\text{red}}^2 \leq 1$, as measured by the entropy. The entropy curves from left to right are for signal-to-noise ratios of 10, 30, 50, 100, 300, and 1000.

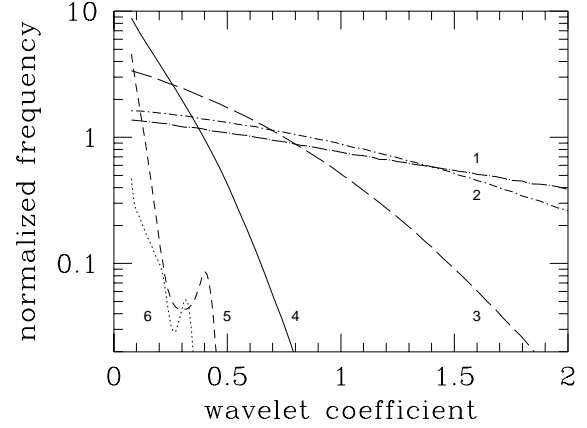


Figure 4. The normalized distribution of the wavelet coefficients at the levels $j = 1 \dots 6$. The coefficients increase in magnitude at the coarser (lower j) resolutions, indicating that they carry most of the information in the spectra.

6. Applying a cut-off in the coefficients corresponding to $\chi_{\text{red}}^2 = 1$ yields for the average number retained of the initially 2^j coefficients for $j = 1 \dots 6$ the respective values 1.9, 3.8, 7.4, 11.6, 6.9, and 3.4. While almost all of the coefficients for $j \leq 3$ are needed, a decreasing fraction is required to describe the spectra at higher resolution.

The distributions are insensitive to the signal-to-noise ratio, as shown in Fig. 5. Except for the lowest ratio of 10, the curves coincide, showing that they may be measured accurately even for a varying signal-to-noise ratio in a spectrum, provided it is not too low.

To demonstrate that the wavelet coefficient distributions may be used to discriminate between different predictions for the statistical properties of the Ly α forest, a second set of Monte Carlo realizations with alternative column density and Doppler parameter distributions is generated. The parameters adopted are those reported by Hu et al. They found that the forest statistics are consistent with an H I column density distribution with a slope of 1.5 for clouds with $12.3 < \log N_{\text{HI}} < 14.5$ and a Gaussian Doppler parameter distribution with mean 28 km s^{-1} , standard deviation 10 km s^{-1} , and a sharp cut-off below 20 km s^{-1} . The resulting average Doppler parameter is 37 km s^{-1} . The simulation is normalized to the same line density per unit redshift at $z = 3$ as found by Hu et al., but the column density distribution is extended to $\log N_{\text{HI}} = 16$ to be consistent with the previous set of simulations. The resulting wavelet coefficient distributions are compared with those from the previous simulation for $j = 3, 4$, and 5 in Fig. 6. The wavelet coefficients are able to distinguish between the two models.

The Kolmogorov–Smirnov test may be used to assess the probability that the wavelet coefficients of a measured spectrum match a given distribution for each resolution level

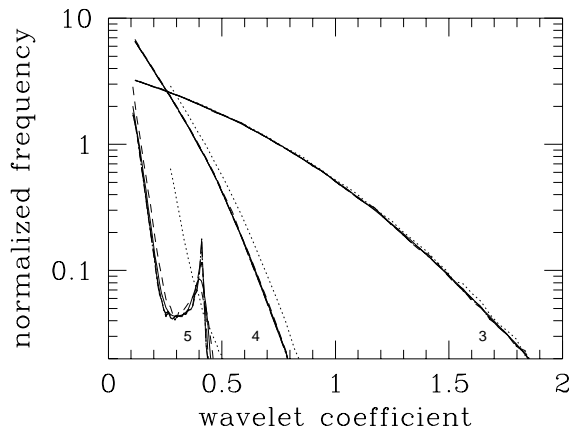


Figure 5. The normalized distribution of the wavelet coefficients for the levels $j = 3, 4$, and 5 for signal-to-noise ratios of 10, 30, 50, 100, 300, and 1000. Except for $S/N = 10$ (dotted lines), the distributions overlap.

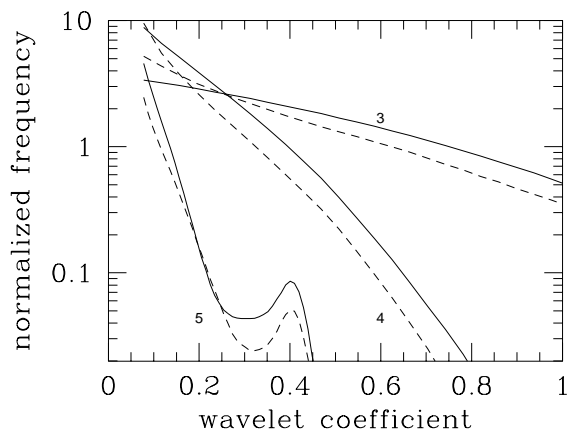


Figure 6. The normalized frequencies of the wavelet coefficients for the levels $j = 3, 4$, and 5 for two different statistical descriptions of the Ly α forest. The solid lines are based on the Voigt parameter distributions inferred by Kirkman & Tytler, and the dashed on the distributions inferred by Hu et al. A signal-to-noise ratio of 50 is used in both sets of simulations. The distributions of wavelet coefficients distinguish between the two models.

j . The most stringent test, however, is given by combining the probabilities for all the distributions. Because any given absorption feature may be expected to affect the coefficients at more than a single resolution level j , it is possible that the coefficients corresponding to a given set of nested blocks for different j (see Fig. 1) may be correlated. In this case, the probabilities of matching the various distributions may not be combined as if they were independent. To determine the degree to which the distributions may be treated as independent, the correlations are measured for coefficients between the various levels j corresponding to the same hierarchy of blocks, and then averaged over all the hierarchies, for a set of Monte Carlo realizations using the fiducial forest model. The results are shown in Table 1. (The level $j = 0$ refers to the correlations with the pair of coefficients corresponding to the course scale averages.) A signal-to-noise ratio of 50 is assumed, and a cut-off in the coefficients is applied to ensure $\chi_{\text{red}}^2 = 1$. The error on the correlations is $\sim 0.1\%$. Although the correlations are small, they are not absent. They are sufficiently small, however, that treating the probabilities for the different distributions as independent should be an adequate approximation for model testing.

2.4 Data compression

One of the key features of wavelets is their ability to compress data. Figs. 2 and 3 show that it is possible to fit a spectrum using only a subset of the wavelets used in its DWT at a statistically acceptable level ($\chi_{\text{red}}^2 = 1$), without significantly degrading the information content of the spectrum as measured by the wavelet entropy. This suggests that filtering the spectrum in this way may provide a usable spectrum that is relatively noiseless and suitable for absorption line fitting.

This is illustrated by performing Voigt profile fitting to Monte Carlo realisations of the fiducial line model, with an assumed signal-to-noise ratio of 50. A wavelet filtered representation of each realised spectrum is generated with coefficients truncated to give a reduced $\chi_{\text{red}}^2 = 1$ for the difference between the original and wavelet filtered spectra. This corresponds on average to retaining only 30% of the full set of coefficients. A representative spectrum is shown in Fig. 7.

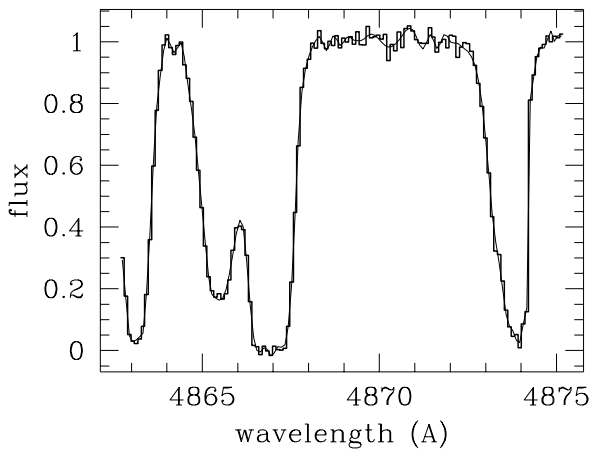
Absorption lines are then identified in the filtered spectrum and fit using AutoVP. The results of 10^4 realisations are shown in Figs. 8 and 9. Also shown are the distributions obtained from AutoVP using the original spectra with no wavelet filtering applied. The distributions are nearly identical. A negligible loss is incurred in the recovery of the line parameters despite the exclusion of 70% of the information in the original spectra.

3 APPLICATION TO Q1937–1009

In this section, the Discrete Wavelet Transform is used to analyse the Ly α forest as measured in the $z = 3.806$ QSO Q1937–1009. The spectrum was taken with the Keck HIRES at a resolution of $\sim 8.5 \text{ km s}^{-1}$ (Burlles & Tytler 1997). The signal-to-noise ratio per pixel was ~ 50 . The spectrum covers the range between Ly α and Ly β in the QSO restframe. (The region analysed is restricted to the redshift interval

Table 1. Wavelet coefficient correlation matrix for resolution levels $j = 6, \dots, 0$.

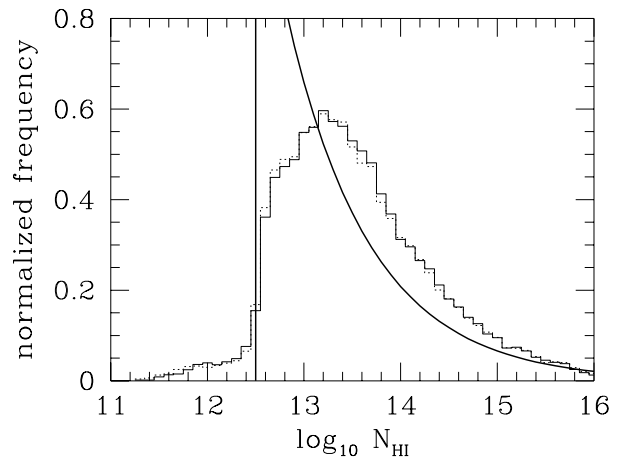
j	6	5	4	3	2	1	0
6	1.000	0.003	0.009	0.013	0.009	0.003	0.001
5	0.003	1.000	-0.020	-0.013	-0.005	-0.001	-0.001
4	0.009	-0.020	1.000	0.026	0.018	0.012	0.000
3	0.013	-0.013	0.026	1.000	0.046	0.025	0.002
2	0.009	-0.005	0.018	0.046	1.000	0.035	0.005
1	0.003	-0.001	0.012	0.025	0.035	1.000	-0.002
0	0.001	-0.001	0.000	0.002	0.005	-0.002	1.000

**Figure 7.** Synthetic spectrum with $S/N = 50$ (heavy solid histogram). The wavelet filtered spectrum with $\chi_{\text{red}}^2 = 1$ is shown by the lighter line (shown as a smooth curve for clarity).

$3.055 < z < 3.726$ to avoid any possible influence by the QSO.)

The distribution of wavelet coefficients is shown in Fig. 10 for $j = 2, 3, 4$, and 5. As in Fig. 4, the high frequency coefficients are generally smaller than at lower frequencies, indicating that the fluctuations that dominate the spectra have been resolved.

The cumulative distributions of the coefficients are compared with the predicted distributions for the fiducial model in Fig. 11. The predicted distributions were generated by simulating spectra with the same pixelization, resolution, signal-to-noise ratio and wavelength coverage as for the measured spectrum of Q1937–1009. An increase in line density per unit redshift proportional to $(1+z)^{2.6}$ (Kirkman & Tytler) was included to match to the redshift range of Q1937–1009. While the distributions generally agree well, a large variation is found for $j = 4$, corresponding to fluctuations on the scale of $17 - 34 \text{ km s}^{-1}$, suggesting some differences from the line model of Kirkman & Tytler. Effects neglected in the simulations that could produce a difference are the presence of metal systems and redshift correlations between the Ly α absorption systems. The changes that would

**Figure 8.** The recovered H I column density distribution from a set of Monte Carlo realizations. The dotted curve corresponds to the Voigt fits obtained using the original unfiltered spectra. The solid curve shows the recovered distribution obtained from the wavelet filtered spectrum for which only 30% of the wavelet coefficients are retained, corresponding to a reduced $\chi_{\text{red}}^2 = 1$ for the difference between the original and wavelet filtered spectra. The heavy solid line shows the input model distribution.

be produced, however, are most likely small: the number of metal systems is small, and the correlations appear weak or absent (Meiksin & Bouchet 1995; Kim et al. 1997). Still, the sensitivity of the wavelet coefficient distributions to these effects may be worth more careful consideration.

4 SUMMARY

Wavelets may be usefully employed to provide a statistical characterization of the absorption properties of the Ly α forest. An approach is presented that performs a multiresolution analysis of the forest using the Discrete Wavelet Transform of the QSO spectrum. The transform decomposes the local frequency dependence of the light fluctuations into an orthogonal hierarchy of basis functions, the wavelets. It is found that in spectra of better than 10 km s^{-1} resolution, most of the information of the spectrum is carried by the

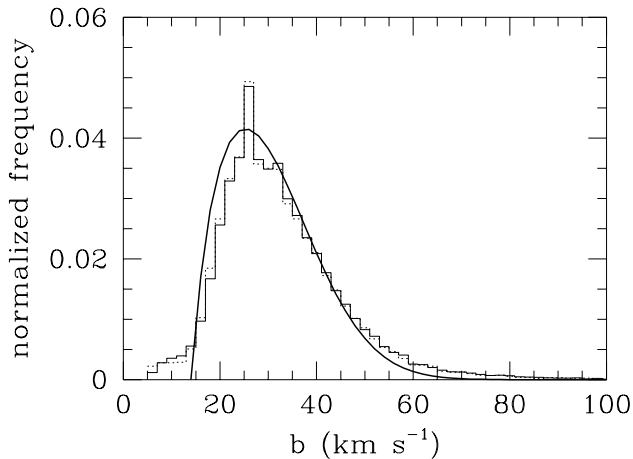


Figure 9. The recovered Doppler parameter distribution, as in Fig. 8. The heavy solid line shows the input model distribution.

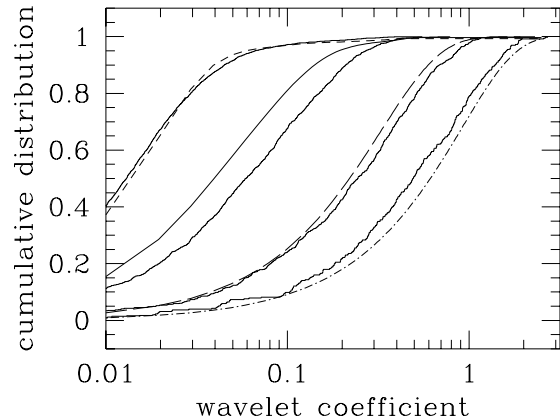


Figure 11. The cumulative distributions of the wavelet coefficients for the spectrum of Q1937–1009, along with the predicted distributions according to the line model of Kirkman & Tytler (1997). The frequency levels shown are $j = 2$ (dot-dashed), $j = 3$ (long-dashed), $j = 4$ (solid), and $j = 5$ (short-dashed).

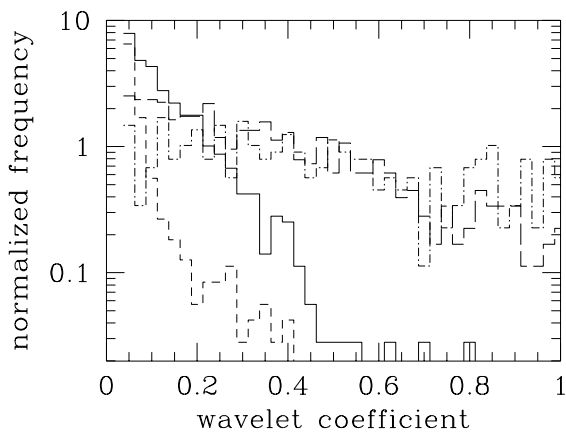


Figure 10. The normalized distributions of the wavelet coefficients for the spectrum of Q1937–1009. The distributions are shown for the levels $j = 2$ (dot-dashed), $j = 3$ (long-dashed), $j = 4$ (solid), and $j = 5$ (short-dashed). The faster decline at higher frequencies demonstrates that the absorption features dominating the spectrum have been adequately resolved.

lower frequency wavelets. For a signal-to-noise ratio typical of even the highest quality spectra ($S/N = 10 - 100$), only 10–30% of the wavelets are required to provide a statistically acceptable description of the spectrum, corresponding to a data compression factor of 3–10. It is shown that a Voigt profile line analysis performed on the wavelet filtered spectra yields nearly identical line parameter distributions as obtained from the original unfiltered spectra.

The distributions of the wavelet coefficients offer an alternative statistical description of the Ly α forest while retaining information on the line widths. It is demonstrated that the correlations of coefficients between different levels in the wavelet hierarchy are weak (a few percent or smaller). Consequently, each of the distributions may be treated as statistically independent to good approximation.

The method is applied to a Keck HIRES spectrum of Q1937–1009. The wavelet coefficient distributions behave qualitatively similarly to those found in Monte Carlo simulations based on the line parameter distributions reported by Kirkman & Tytler. The measured distributions, however, show some differences on the scale $17 - 34 \text{ km s}^{-1}$.

The results demonstrate that Multiresolution Analysis using the Discrete Wavelet Transform provides an alternative objective, easily automated procedure for analysing the Ly α forest suitable for basing a comparison between the measured properties of the Ly α forest and the predictions of numerical models.

The author thanks S. Burles and D. Tytler for kindly providing the spectrum of Q1937–1009, and R. Davé for permission to use AutoVP.

REFERENCES

- Berkooz G., Holmes P., Lumley J. L., 1993, *Ann. Rev. Fluid Mech.*, 25, 539
- Bond J. R., Wadsley J. W., 1997, in Petitjean, P., Charlot, S., eds, *Proc. 13th IAP Astro. Colloq., Structure and Evolution of the Intergalactic Medium from QSO Absorption Line Systems*. Editions Frontières, Paris, p. 143
- Burles S., Tytler D., 1997, *AJ*, 114, 1330
- Cen R., Miralda-Escudé J., Ostriker J. P., Rauch M., 1994, *ApJ*, 437, L9
- Chui C. K., 1992, *An Introduction to Wavelets*. Academic Press, San Diego
- Daubechies I., 1992, *Ten Lectures on Wavelets*. SIAM, Philadelphia
- Davé R., Hernquist L., Weinberg D. H., Katz N., 1997, *ApJ*, 477, 21
- Hernquist L., Katz N., Weinberg D., Miralda-Escudé J., 1996, *ApJ*, 457, L51
- Hu E. M., Kim T. S., Cowie L. L., Songaila A., Rauch M., 1995, *AJ*, 110, 1526
- Kim T.-S., Hu E. M., Cowie L. L., Songaila A., 1997, *AJ*, 114, 1
- Kirkman D., Tytler D., 1997, *ApJ*, 484, 672
- Lynds R., 1971, *ApJ*, 164, L73
- Machacek M. E., Bryan G. L., Meiksin A., Anninos P., Thayer D., Norman M., Zhang Y., 2000, *ApJ* (in press)
- Meiksin A., Bouchet F. R., 1995, *ApJ*, 448, L85
- Meiksin A. et al., 2000, in preparation
- Meyer Y., 1993, *Wavelets: Algorithms and Applications*. SIAM, Philadelphia
- Miralda-Escudé J., Cen R., Ostriker J. P., Rauch M., 1996, *ApJ*, 471, 582
- Pando J., Fang L.-Z., 1996, *ApJ*, 459, 1
- Press W. H., Teukolsky, S. A., Vetterling, W. T., Flannery, B. P., 1992, *Numerical Recipes*, 2nd edn. Cambridge Univ. Press, Cambridge
- Sargent W. L. W., Young P. J., Boksenberg A., Tytler D., 1980, *ApJS*, 42, 41
- Slezak E., Bijaoui A., Mars G., 1990, *AA*, 227, 301
- Theuns T., Leonard A., Efstathiou G., 1998, *MNRAS*, 297, L49
- Zhang Y., Anninos P., Norman M. L., 1995, *ApJ*, 453, L57
- Zhang Y., Anninos P., Norman M. L., Meiksin A., 1997, *ApJ*, 485, 496
- Zhang Y., Meiksin A., Anninos P., Norman, M. L., 1998, *ApJ*, 495, 63
- Zuo L., Bond J. R. 1994, *ApJ*, 423, 73

